




# Pretreatment PET/CT imaging of angiogenesis based on $^{18}\text{F}$ -RGD tracer uptake may predict antiangiogenic response

Li Li<sup>1,2</sup> · Li Ma<sup>2</sup> · Dongping Shang<sup>2</sup> · Zhiguo Liu<sup>2</sup> · Qingxi Yu<sup>2</sup> · Suzhen Wang<sup>2</sup> · Xuepeng Teng<sup>2</sup> · Qiang Zhang<sup>3</sup> · Xudong Hu<sup>2,4</sup> · Wei Zhao<sup>2</sup> · Wenhong Hou<sup>2</sup> · Jianyue Jin<sup>5</sup> · Feng-Ming (Spring) Kong<sup>6</sup> · Jinming Yu<sup>2</sup> · Shuanghu Yuan<sup>2,4</sup> 

Received: 7 April 2018 / Accepted: 19 August 2018 / Published online: 5 September 2018  
© Springer-Verlag GmbH Germany, part of Springer Nature 2018

## Abstract

**Purpose** To explore the relationship between metabolic uptake of the  $^{18}\text{F}$ -ALF-NOTA-PRGD<sub>2</sub> ( $^{18}\text{F}$ -RGD) tracer on positron emission tomography/computerized tomography (PET/CT) and the antiangiogenic effect of apatinib in patients with solid malignancies.

**Materials and patients** Patients with measurable lesions scheduled for second- or third-line single-agent therapy with apatinib were eligible for this prospective clinical trial. All patients underwent  $^{18}\text{F}$ -RGD PET/CT examination before the start of treatment. Standardized uptake values (SUVs) of contoured tumor lesions were computed and compared using independent sample *t*-tests or the Mann–Whitney U test. Receiver-operating characteristic (ROC) curve analysis was used to determine accuracy in predicting response. Survival curves were compared using the Kaplan–Meier method.

**Results** Of 38 patients who consented to study participation, 25 patients with 42 measurable lesions met the criteria for inclusion in this response assessment analysis. The median follow-up time was 3 months (range, 1–10 months), and the median progression-free survival (PFS) was 3 months (95% confidence interval, 1.04–4.96). The SUV<sub>peak</sub> and SUV<sub>mean</sub> were significantly higher in responding tumors than in non-responding tumors ( $4.98 \pm 2.34$  vs  $3.59 \pm 1.44$ ,  $p = 0.048$ ;  $3.71 \pm 1.15$  vs  $2.95 \pm 0.49$ ,  $P = 0.036$ ). SUV<sub>max</sub> did not differ between responding tumors and non-responding tumors ( $6.58 \pm 3.33$  vs  $4.74 \pm 1.83$ ,  $P = 0.078$ ). An exploratory ROC curve analysis indicated that SUV<sub>mean</sub> [area under the ROC curve (AUC) = 0.700] was a better parameter than SUV<sub>peak</sub> (AUC = 0.689) for predicting response. Using a threshold value of 3.82, high SUV<sub>mean</sub> at baseline was associated with improved PFS (5.0 vs. 3.4 months, log-rank  $P = 0.036$ ).

**Conclusion**  $^{18}\text{F}$ -RGD uptake on PET/CT imaging pretreatment may predict the response to antiangiogenic therapy, with higher  $^{18}\text{F}$ -RGD uptake in tumors predicting a better response to apatinib therapy.

**Keywords** Antiangiogenic therapy · Malignancies ·  $^{18}\text{F}$ -RGD PET/CT · Integrin  $\alpha\beta 3$

## Background

Angiogenesis, the process of new blood vessel formation from preexisting vessels, is largely regulated by interactions between vascular endothelial growth factors (VEGFs) and VEGF receptors (VEGFRs) [1, 2]. In the context of cancer, the process of angiogenesis becomes uncontrolled, leading to pathological over-formation of blood vessels. Various types of angiogenesis inhibitors have shown clinical benefit in many types of cancers [3, 4], but treatment efficacies of anti-angiogenic therapies are heterogeneous among different patients. Several clinical trials have explored biomarkers that can effectively predict the response to antiangiogenic therapy, but no clinical data are available yet on this subject [5, 6]. Moreover, antiangiogenic drugs, such as the VEGF antibody bevacizumab, are commonly

✉ Shuanghu Yuan  
yuanshuanghu@sina.com

<sup>1</sup> School of Medicine and Life Sciences, University of Jinan–Shandong Academy of Medical Sciences, Jinan, Shandong, China  
<sup>2</sup> Department of Radiation Oncology, Shandong Cancer Hospital and Institute–Shandong Cancer Hospital Affiliated to Shandong University, No 440 Jiyan Road, Jinan 250117, Shandong, China  
<sup>3</sup> Zibo Forth People’s Hospital, Zibo, Shandong, China  
<sup>4</sup> Shandong Academy of Medical Sciences, Jinan, Shandong, China  
<sup>5</sup> Department of Radiation Oncology, Indiana University School of Medicine, Indianapolis, IN, USA  
<sup>6</sup> Department of Radiation Oncology, Simon Cancer Center, Indiana University School of Medicine, Indianapolis, IN, USA

applied in combination with conventional chemotherapy or radiotherapy [7, 8], and this combined treatment model may confound the ability to identify reliable biomarkers for the response to antiangiogenic therapy.

Alpha v beta3 ( $\alpha v\beta 3$ ), which forms complexes with VEGFRs, is considered to be the most important integrin in the process of angiogenesis, and is highly expressed on newly formed vessels [9–11]. Because the tripeptide moiety of arginine–glycine–aspartate (RGD) can specifically bind to integrin  $\alpha v\beta 3$ , RGD positron emission tomography/computerized tomography (PET/CT) has been suggested for noninvasive imaging of angiogenesis [12–14]. A novel tracer  $^{18}\text{F}$ -AIF-NOTA-PRGD2 (denoted as  $^{18}\text{F}$ -RGD) has been proven to offer clinically simple and safe imaging of  $\alpha v\beta 3$  expression using a simple, one-step lyophilized kit [15]. Therefore, we hypothesized that  $^{18}\text{F}$ -RGD PET/CT can provide a useful tool for predicting the response to antiangiogenic therapy, and we tested this hypothesis in the context of treatment with apatinib (YN968D1), the first orally antiangiogenic drug targeting the VEGFR-2 tyrosine kinase that can be used in single-agent treatment [16].

## Patients and methods

### Patients

For this institutional ethics committee-approved prospective study, patients scheduled for second- or third-line apatinib therapy were recruited, and those who signed consent forms were prospectively enrolled. Cases of locally advanced and metastatic malignancies confirmed by histologic analysis were eligible. Other eligibility criteria included: age at least 18 years and Karnofsky performance status (KPS) of at least 70. Patients who did not have measurable lesions, were pregnant or unable to complete the required examinations were excluded. The study was reported to [ClinicalTrials.gov](https://clinicaltrials.gov) (NCT03384511, CRTOG1701).

### Study drug dosing and treatment

All patients were treated with the following regimen: apatinib 250 mg twice daily (500 mg/day). A treatment cycle was defined as 4 weeks, and treatment interruptions or dose reductions to 250 mg per day were allowed for the management of adverse events (AEs). The maximum allowable period of treatment interruption was 1 week during each cycle. The dose had to be re-escalated to 500 mg per day after the mitigation of the AE. The treatment was not stopped until disease progression, intolerable toxicity, or patients' request for withdrawal from the study.

## $^{18}\text{F}$ -RGD PET/CT imaging

All  $^{18}\text{F}$ -RGD PET/CT scans were performed using a combined PET/CT scanner (GEMINI TF Big Bore; Philips Healthcare) within 3 days prior to the start of apatinib treatment. The lyophilized kit for labeling the PRGD<sub>2</sub> peptide was purchased from Jiangsu Institute of Nuclear Medicine, and  $^{18}\text{F}$ -RGD was prepared as previously described [15]. The radiochemical purity of  $^{18}\text{F}$ -RGD exceeded 95%, and its specific radioactivity exceeded 37 GBq (1000 mCi)/ $\mu\text{mol}$ . PET images were obtained from the head to the thigh for 5 min per field of view, with an axial sampling thickness of 4.25 mm per slice after intravenous administration of  $^{18}\text{F}$ -RGD. The patients were instructed to breathe slowly and shallowly during PET acquisition. The images were attenuation corrected with the transmission data from CT. The attenuation-corrected PET images, CT images, and fused PET/CT images displayed as coronal, sagittal, and transaxial slices were viewed on a Xeleris work station (GE Healthcare).

### Image analysis

The PET/CT images were analyzed by two experienced nuclear medicine physicians using MIM software (MIM, 6.1.0, Cleveland, OH, USA) to determine the uptake in tumor lesions. To guarantee the accuracy of regions of interest (ROIs) over lesions, ROIs were drawn with reference to anatomical structure adjusted by CT images and PET/CT fusion images. The peak, maximum, and mean standardized uptake values ( $\text{SUV}_{\text{peak}}$ ,  $\text{SUV}_{\text{max}}$ , and  $\text{SUV}_{\text{mean}}$ ) of lesions were processed with an automated contouring program, using a threshold SUV of 2.5 [17].

### Response evaluation

Treatment responses were assessed by measuring changes in the largest diameter of each tumor from pretreatment PET/CT to post-treatment CT. The percentage change was calculated using the following formula:  $\% \text{ change} = (\text{Diameter}_{\text{post}} - \text{Diameter}_{\text{pre}}) / \text{Diameter}_{\text{pre}} \times 100\%$ . Lesions were classified as responding tumors if the  $\% \text{ change}$  was  $> 30\%$  or non-responding tumors if the  $\% \text{ change}$  was  $< 30\%$ . Progression-free survival (PFS) was defined as the time from the start of apatinib therapy to disease progression or death due to any cause, whichever occurred first.

### Statistical analysis

All statistical analysis was performed using SPSS version 21.0 (SPSS, Inc., Chicago, IL, USA). Differences in SUV values of lesions were analyzed using independent sample *t*-tests. The Mann–Whitney U test was used for data that did not show a normal distribution. Receiver-operating characteristic (ROC) curve analysis was used to determine accuracy in predicting response. Survival curves were compared using the Kaplan–

Meier method. Probability values < 0.05 were considered indicative of significant differences.

## Results

### Demographic and clinical characteristics of patients

From September 2016 to September 2017, 38 patients for whom single-agent treatment with apatinib was planned consented to participation in the study. All patients underwent  $^{18}\text{F}$ -RGD PET/CT imaging examination pretreatment. Thirteen patients were excluded from the antiangiogenic response analysis; two of these refused apatinib therapy, five received apatinib therapy for < 4 weeks (one treatment cycle), two received combined chemoradiation during the first cycle of apatinib treatment, and four did not complete the 1-month follow-up scan. Consequently, 25 patients with 42 measurable lesions were included in the response analysis. The characteristics of patients and tumor are summarized in Table 1.

### Response to apatinib treatment

At the time of this analysis, the median follow-up time was 3 months (range, 1–10 months), and the median PFS was 3 months [95% confidence interval (CI), 1.04–4.96]. After the first cycle (4 weeks) of apatinib therapy, 14 lesions showed a reduction in diameter of > 30% and were considered to be responding tumors, and the remaining 28 lesions were considered non-responding tumors. The median PFS of patients in the responding and non-responding groups were 5.0 and

3.4 months respectively (log-rank,  $P = 0.009$ ). The  $^{18}\text{F}$ -RGD PET/CT uptake values and treatment responses in the 42 measurable lesions are shown in Table 2.

### $^{18}\text{F}$ -RGD uptake values in different types of tumors

No significant differences were observed in the  $\text{SUV}_{\text{peak}}$ ,  $\text{SUV}_{\text{max}}$  and  $\text{SUV}_{\text{mean}}$  values for lung cancer, ovarian cancer, cervical cancer, and other lesions ( $4.18 \pm 2.42$  vs  $5.41 \pm 1.53$  vs  $3.60 \pm 1.33$  vs  $3.82 \pm 1.45$ ,  $P = 0.419$ ;  $5.73 \pm 3.32$  vs  $7.21 \pm 1.83$  vs  $4.49 \pm 1.94$  vs  $4.97 \pm 1.71$ ,  $P = 0.279$ ; and  $3.31 \pm 1.08$  vs  $4.00 \pm 0.89$  vs  $2.93 \pm 0.58$  vs  $3.20 \pm 0.84$ ,  $P = 0.134$ ; Fig. 1).

### Correlation between response to antiangiogenic therapy and pretreatment $^{18}\text{F}$ -RGD uptake values

The pretreatment  $^{18}\text{F}$ -RGD uptake values as determined by the two observers are listed in Table 3. The  $\text{SUV}_{\text{peak}}$  and  $\text{SUV}_{\text{mean}}$  were significantly higher in responding tumors than in non-responding tumors (Table 3 and Fig. 2). The difference in the  $\text{SUV}_{\text{max}}$  between responding tumors and non-responding tumors was not significant (Table 3). An exploratory ROC curve comparison was performed to determine the diagnostic accuracy of  $\text{SUV}_{\text{peak}}$  and  $\text{SUV}_{\text{mean}}$  for identifying responding tumors. Compared with the  $\text{SUV}_{\text{peak}}$  [area under curve (AUC) = 0.689], the  $\text{SUV}_{\text{mean}}$  (AUC = 0.700) was a better parameter for predicting response according to the ROC curve analysis (Fig. 3).

According to ROC curve analysis, the threshold value for  $\text{SUV}_{\text{mean}}$  pretreatment was 3.82 for the response of apatinib treatment. The objective response rate (OPR) was 85.7% in lesions with a  $\text{SUV}_{\text{mean}} > 3.82$ , and 22.9% in lesions with a  $\text{SUV}_{\text{mean}} < 3.82$ . Patients whose lesions had a higher  $\text{SUV}_{\text{mean}}$  exhibited better PFS than those whose lesions had a low  $\text{SUV}_{\text{mean}}$  (5.0 vs 3.4 months, log-rank  $P = 0.036$ ; Fig. 4).

## Discussion

Treatments aimed at blocking angiogenesis are commonly used in cancer therapy; however, no clinically identified biomarker is available for predicting the likelihood of response to such therapy. In this study, we provided the first clinical evidence that tumor  $^{18}\text{F}$ -RGD uptake parameters at baseline are predictive for treatment response to apatinib, an oral antiangiogenic drug. Patients whose tumors showed a higher  $\text{SUV}_{\text{mean}}$  had a better response to treatment and longer PFS than those whose tumors showed a lower  $\text{SUV}_{\text{mean}}$ .

Several studies have reported the preclinical use of RGD peptide tracers, and have indicated that a significant decrease in the amount of tracer present can be observed from pre- to post-antiangiogenic therapy [18–22]. Moreover, changes in RGD uptake decreased more obviously in groups treated with

**Table 1** Characteristics of patients and tumors

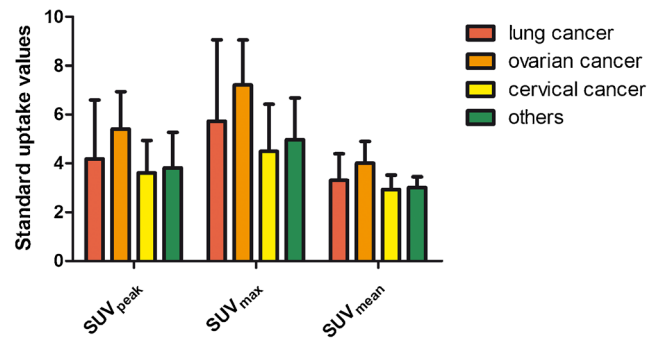
Characters	
Age (years), median (range)	54 (27–78)
Gender, <i>n</i>	
Male	11
Female	14
Smoking, <i>n</i>	
Yes	5
No	20
KPS, median (range)	80 (75–90)
Primary tumors, <i>n</i>	
Lung cancer	9
Esophageal cancer	2
Breast cancer	1
Cervical cancer	5
Ovary cancer	3
Stomach cancer	1
Others	4

**Table 2** Pre-treatment <sup>18</sup>F-RGD PET uptake and % change in tumor size in response to anti-angiogenic therapy in 42 measurable lesions

Patient no.	Primary tumors	Stage	Pathological type	Lesion no.	Pretreatment <sup>18</sup> F-RDG PET uptake			Tumor dimensions, cm		% change	
					SUV <sub>peak</sub>	SUV <sub>max</sub>	SUV <sub>mean</sub>	Baseline	1-month		
#1	Lung cancer	cT2N3M1b IV	Adenocarcinoma	#1	4.64	6.09	3.22	5.4 * 4.4	4.5 * 4.2	-11.2	
#2	Gall bladder cancer	pT3N2M0 IVb	Adenocarcinoma	#2	6.11	7.99	3.67	2.6 * 1.6	2.2 * 1.5	-11.9	
#3				2.74	3.88	2.73	1.3 * 1.0	1.1 * 1.0	-8.6		
#4				2.59	3.82	2.46	1.0 * 1.0	1.9 * 1.4	6.5		
#5				5.81	8.35	4.15	2.2 * 2.0	1.4 * 1.2	-38.1		
#6	Ovarian cancer	cT3N1M1 IV	Adenocarcinoma	#6	5.02	6.94	3.93	2.1 * 1.0	0 * 0	-100	
#4	Esophageal cancer	cT4N1M0 IIIc	Squamous cell carcinoma	#7	4.64	6	3.06	3.0 * 2.8	2.3 * 1.5	-34.5	
#5	Lung cancer	cT3N2M1 IV	Adenocarcinoma	#8	10.27	13.77	5.12	6.5 * 5.5	3.0 * 2.8	-51.7	
#6	Cervical cancer	cT1N1M1 IV	Squamous cell carcinoma	#9	4.56	5.26	3.28	2.6 * 2.2	3.0 * 2.9	-22.9	
#7	Ovarian cancer	pT2N1M0 IIIc	Adenocarcinoma	#10	7.23	8.41	5.52	1.2 * 0.7	0.7 * 0.5	-36.8	
#8	Lung cancer	cT2N2M1 IV	Adenocarcinoma	#11	7.43	12.07	5.49	5.9 * 4.0	2.8 * 2.5	-46.5	
#12	Cervical cancer	cT1N1M1 IV	Squamous cell carcinoma	#12	7.23	8.82	5.05	2.7 * 1.6	1.6 * 1.2	-34.9	
#9				#13	3.69	4.77	3.03	1.6 * 0.5	2.0 * 1.1	47.6	
#14				#14	6.99	9.6	4.21	2.1 * 1.5	2.2 * 1.9	13.9	
#10				#15	5.69	7.41	3.71	2.5 * 1.0	2.3 * 0.9	-8.5	
#11				#16	2.5	3.12	2.74	4.4 * 3.2	0.5 * 0	-93.4	
#12				#17	2.55	3.62	2.68	4.7 * 2.4	3.2 * 1.4	-35.2	
#13				#18	2.9	3.44	2.64	6.9 * 3.7	5.2 * 2.7	-25.5	
#14	Lung cancer	cT2N3M0 IIIB	Adenocarcinoma	#19	4.21	6.76	2.96	5.6 * 3.1	5.5 * 3.7	-11.5	
#20	Lung cancer	cT2N1M1 IV	Adenocarcinoma	#20	2.54	3.27	2.53	5.2 * 3.0	4.9 * 3.6	-3.7	
#21				#21	1.49	2.78	2.34	3.5 * 3.4	5.0 * 3.3	20.2	
#22				#22	3.19	3.78	2.68	1.4 * 1.2	1.2 * 1.1	-11.5	
#23				#23	2.08	3.08	2.37	1.5 * 1.4	1.4 * 1.2	-10.1	
#24				#24	2.34	4.2	2.72	2.2 * 1.1	2.1 * 1.0	-6.1	
#25				#25	3.56	4.74	2.88	5.8 * 5.6	4.4 * 3.4	-31.6	
#26				#26	3.72	4.45	3.06	1.9 * 1.2	1.5 * 0.6	-32.3	
#27				#27	2.5	3.29	2.91	4.1 * 3.2	3.0 * 1.7	-35.6	
#28				#28	3.19	3.63	2.3	1.2 * 1.7	1.0 * 0.7	-41.4	
#29				#29	2.78	3	2.16	1.1 * 1.0	1.1 * 0.8	-9.7	
#19	Nasopharyngeal carcinoma	cTXN1M1 IV	Sarcoma	#30	2.94	4.04	3.03	2.2 * 1.0	1.4 * 1.2	-18.7	
#31	Breast cancer	pT2N1M0 IIb	Others	#31	2.57	3.27	2.65	1.9 * 1.6	2.05 * 1.4	1.2	
#20				#32	3	3.97	2.61	2.61	1.7 * 0.8	3.7 * 1.7	54.1
#21				#33	3.32	4.46	2.85	9.6 * 5.7	7.9 * 5.0	-15.7	
#21	Soft tissue tumor	cT2N0M1 IV	Sarcoma	#34	4.75	5.73	3.32	1.8 * 1.5	2.1 * 1.6	12.1	

Table 2 (continued)

Patient no.	Primary tumors	Stage	Pathological type	Lesion no.	Pretreatment <sup>18</sup> F-RGD PET uptake				Tumor dimensions, cm		% change
					SUV <sub>peak</sub>	SUV <sub>max</sub>	SUV <sub>mean</sub>	Baseline	1-month		
#22	Lung cancer	cT3N2M1 IV	Squamous cell carcinoma	#35	4	4.97	2.99	12.4 * 6.5	7.1 * 6.0	-30.6	
#23	Stomach cancer	cT1N2M1 IV	Others	#36	2.38	2.98	2.63	1.8 * 1.0	2.0 * 1.1	10.7	
#24	Cervical cancer	cT1N1M0 IIIb	Squamous cell carcinoma	#37	2.97	3.36	2.84	1.1 * 0.9	1.7 * 1.1	40	
				#38	2.49	3.42	2.59	2.3 * 1.5	2.3 * 1.9	10.5	
				#39	2.85	3.82	3.05	1.8 * 1.7	1.8 * 1.4	-8.6	
				#40	3.61	4.55	3.24	2.1 * 1.0	1.7 * 1.0	-12.9	
#25	Submandibular gland carcinoma	cTXNXM1 IV	Adenocarcinoma	#41	6.99	8.53	3.69	1.3 * 1.2	2.4 * 1.4	34.2	
				#42	4.18	5.58	3.46	1.0 * 1.0	1.9 * 1.2	35.4	

Fig. 1 Standard uptake values on <sup>18</sup>F-RGD PET/CT in different types of tumors

antiangiogenic drugs than in those treated with vehicle control, and these changes occurred much earlier than the fluorodeoxyglucose (FDG) metabolic response [18, 19]. These observations confirmed the feasibility of using RGD to monitor early biological changes and efficacy during antiangiogenic therapy. In a previous study with bevacizumab-containing therapy in ovarian and cervical cancers, the decrease in RGD uptake was also observed, and a large decrease in the SUV<sub>mean</sub> was noted in patients who had an objective response in the early observation of response [23]. However, that study only assessed the change ratios rather than baseline uptake levels and, therefore, could not determine whether RGD uptake could be used to predict response and screen appropriate patients for treatment decision-making. Also, because patients in that study were given the combination therapy, it is not possible to identify the relationship between response and antiangiogenic therapy directly.

In this trial, we applied single-agent treatment with apatinib, and both the baseline SUV<sub>peak</sub> and SUV<sub>mean</sub> were found to be predictors of response, with a higher SUV<sub>mean</sub> also being significantly correlated with prolonged PFS. To our knowledge, this is the first systemic clinical investigation of correlations between RGD uptake parameters and response in various types of malignant tumors. Inhibition of  $\alpha v \beta 3$  integrin activity has been shown to induce apoptosis among tumor endothelial cells and to effectively inhibit tumor angiogenesis and progression [24–26]. Cheresh et al. reported that decreased expression of  $\alpha v \beta 3$  on  $\alpha v \beta 3$ -bearing endothelial cells seeded in a three-dimensional collagen matrix prolonged their survival [27, 28]. Consequently, higher RGD uptake values may indicate a high density of effective target receptors for antiangiogenic therapy, and predict a better response to apatinib therapy.

<sup>18</sup>F-RGD uptake on PET/CT as a biomarker seems to behave differently according to the treatment modality. Previous studies investigating the utility of <sup>18</sup>F-RGD PET/CT were mostly carried out in patients treated with antiangiogenic drugs in combined therapies. Our previous studies on non-small cell lung cancer and glioblastoma found that high

**Table 3** Parameters of pretreatment <sup>18</sup>F-RGD PET/CT scans

Parameters	All lesions	Responding tumors	Non-responding tumors	<i>P</i>
SUV <sub>peak</sub>	4.05 ± 1.88	4.98 ± 2.34	3.59 ± 1.44	0.048
SUV <sub>max</sub>	5.36 ± 2.55	6.58 ± 3.33	4.74 ± 1.83	0.078
SUV <sub>mean</sub>	3.20 ± 0.84	3.71 ± 1.15	2.95 ± 0.49	0.036

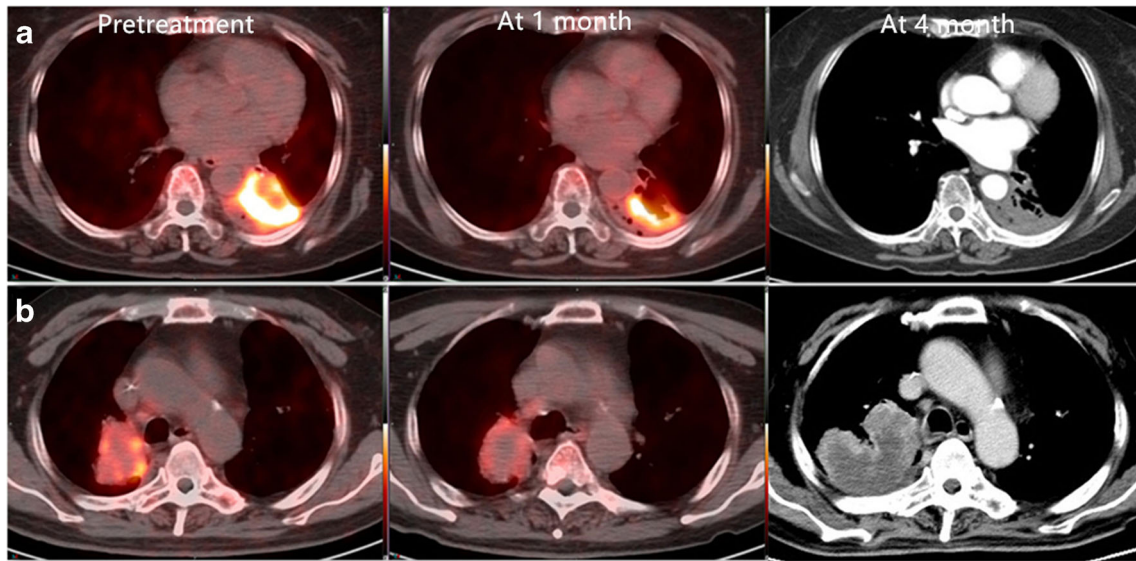


**Fig. 2** Two representative <sup>18</sup>F-RGD PET/CT scans of responding tumors (**a**: SUV<sub>mean</sub> = 5.12) and non-responding tumors (**b**: SUV<sub>mean</sub> = 3.67). (*Top panel*) Scans from a patient with active RGD uptake at baseline

and during treatment who showed a good response to apatinib treatment, and (*bottom panel*) scans from another patient with remarkable tumor progression

**Fig. 3** ROC curve for the accuracy of <sup>18</sup>F-RGD PET/CT parameters to predict response to apatinib treatment

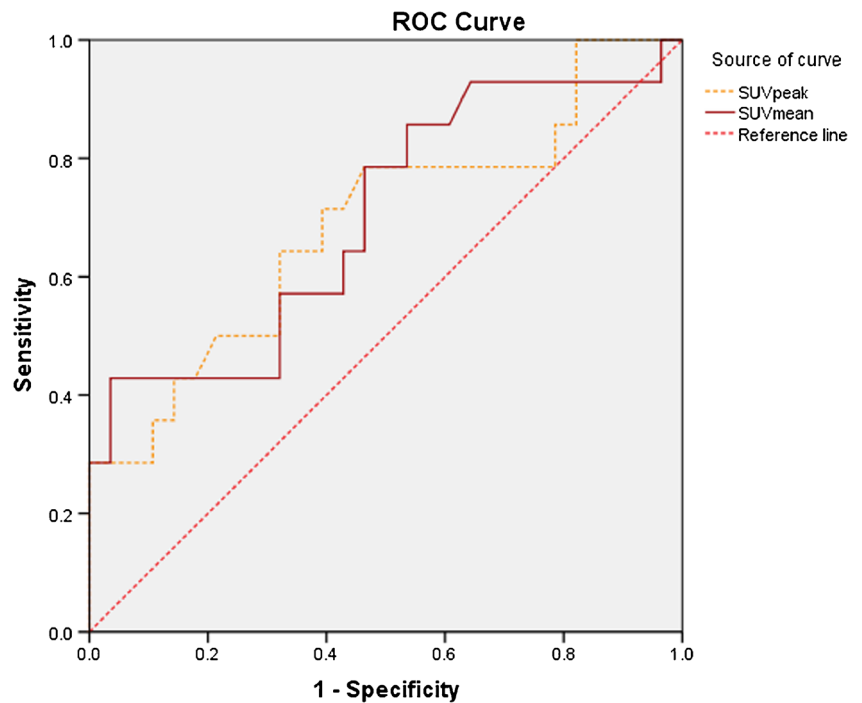
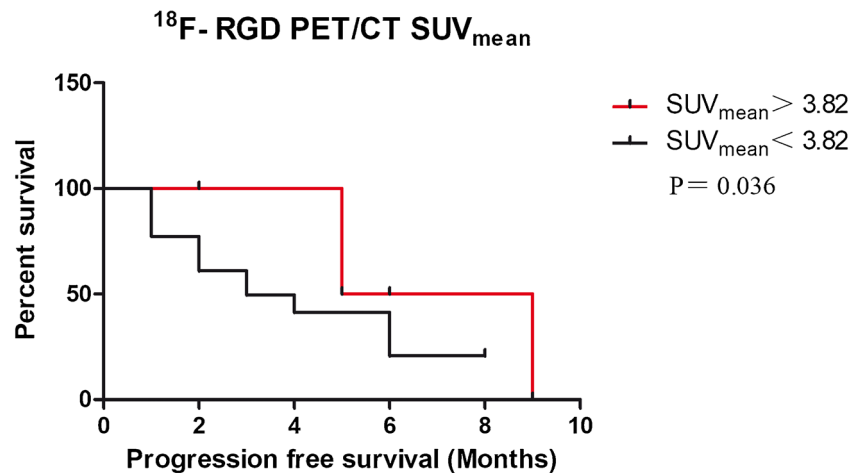


**Fig. 4** Kaplan–Meier analysis of PFS for patients whose lesions showed differing amounts of  $^{18}\text{F}$ -RGD uptake



RGD uptake values indicated a poor outcome after concurrent chemoradiation therapy (CCRT) [17, 29]. During CCRT, high RGD uptake values indicated high malignancy and severe hypoxia, which were associated with rapid progression and increased chemoradiation resistance in tumors [17, 30]. Discrepancies in the relationship between  $^{18}\text{F}$ -RGD uptake and response to therapy may be the result of different implications of  $\alpha v \beta 3$  in different treatment modalities.

To our knowledge, this is the first clinical trial to demonstrate  $^{18}\text{F}$ -RGD uptake on PET/CT as an imaging biomarker to predict treatment response to antiangiogenic treatment. If validated in a larger sample in an external study,  $^{18}\text{F}$ -RGD PET/CT will provide references for the planning of personalized, targeted antiangiogenic therapy in various cancers. Given the small number of patients and the disunity of tumors in the present study, we will continue to increase the sample size and further identify the potential ability of  $^{18}\text{F}$ -RGD PET/CT to predict the response to antiangiogenic therapy in multi-center studies.

## Conclusions

The results of the present study indicate that  $^{18}\text{F}$ -RGD PET/CT may be applied to predict the response to antiangiogenic therapy, with high RGD uptake values in tumors predicting a better response to apatinib therapy.

**Acknowledgments** The authors would like to thank Ms. Laney Weber for excellent assistance.

**Funding** This study was partially funded by Shandong Key Research and Development Plan (2017CXGC1209 and 2017GSF18164) and the Outstanding Youth Natural Science Foundation of Shandong Province (JQ201423), Jinan Clinical Medicine Science and Technology Innovation Plan (201704095), NSFC81372413, National Key Research and Development Program of China (2016YFC0904700).

## Compliance with ethical standards

**Conflict of interest** The authors declare no potential conflicts of interest.

**Ethical standards** Our investigation was approved by the Shandong Cancer Hospital affiliated to Shandong University Ethical Committee. All persons gave their informed consent prior to their inclusion in the study.

## References

- Folkman J. The role of angiogenesis in tumor growth. *Semin Cancer Biol.* 1992;3:65–71.
- Longo R, Gasparini G. Challenges for patient selection with VEGF inhibitors. *Cancer Chemother Pharmacol.* 2007;60:151–70.
- Eskens FA. Angiogenesis inhibitors in clinical development; where are we now and where are we going. *Br J Cancer.* 2004;90:1–7.
- Abdelrahim M, Konduri S, Basha R, Philip PA, Baker CH. Angiogenesis: an update and potential drug approaches (review). *Int J Oncol.* 2010;36:5–18.
- U.S. National Library of Medicine (2009–2012) Efficacy study of [F-18]RGD-K5 positron emission tomography (PET) as a tool to monitor response to an anti-angiogenic drug. *ClinicalTrials.gov Identifier: NCT00988936.* Sponsor: Siemens Molecular Imaging
- Winick J (2007) A proof-of-concept study to assess the ability of [18F]AH-111585 PET imaging to detect tumours and angiogenesis. *ClinicalTrials.gov*; November 28, 2007 ed. US: National Institutes of Health; 2007.
- Kerbel RS. Antiangiogenic therapy: a universal chemosensitization strategy for cancer. *Science.* 2006;312:1171–5.
- Hurwitz H, Fehrenbacher L, Novotny W, Cartwright T, Hainsworth J, Heim W, et al. Bevacizumab plus irinotecan, fluorouracil, and leucovorin for metastatic colorectal cancer. *N Engl J Med.* 2004;350:2335–42.
- Ruoslahti E. Specialization of tumour vasculature. *Nat Rev Cancer.* 2002;2:83–90.
- Liu Z, Wang F, Chen X. Integrin  $\alpha(v)\beta(3)$ -targeted cancer therapy. *Drug Dev Res.* 2008;69:329–39.
- Danhier F, Le BA, Preat V. RGD-based strategies to target  $\alpha(v)\beta(3)$  integrin in cancer therapy and diagnosis. *Mol Pharm.* 2012;9:2961–73.
- Beer AJ, Haubner R, Wolf I, Goebel M, Luderschmidt S, Niemeyer M, et al. PET-based human dosimetry of  $^{18}\text{F}$ -galacto-RGD, a new

- radiotracer for imaging alpha v beta3 expression. *J Nucl Med.* 2006;47:763–9.
13. Xiong JP, Stehle T, Zhang R, Joachimiak A, Frech M, Goodman SL, et al. Crystal structure of the extracellular segment of integrin alpha Vbeta3 in complex with an Arg-Gly-Asp ligand. *Science.* 2002;296:151–5.
  14. Yu YP, Wang Q, Liu YC, Xie Y. Molecular basis for the targeted binding of RGD-containing peptide to integrin alphaVbeta3. *Biomaterials.* 2014;35:1667–75.
  15. Wan W, Guo N, Pan D, Yu C, Weng Y, Luo S, et al. First experience of 18F-alfatide in lung cancer patients using a new lyophilized kit for rapid radiofluorination. *J Nucl Med.* 2013;54:691–8.
  16. Fontanella C, Ongaro E, Bolzonello S, Guardascione M, Fasola G, Aprile G. Clinical advances in the development of novel VEGFR2 inhibitors. *Ann Transl Med.* 2014;2:123.
  17. Luan X, Huang Y, Gao S, Sun X, Wang S, Ma L, et al. (18)F-alfatide PET/CT may predict short-term outcome of concurrent chemoradiotherapy in patients with advanced non-small cell lung cancer. *Eur J Nucl Med Mol Imaging.* 2016;43:2336–42.
  18. Shi J, Jin Z, Liu X, Fan D, Sun Y, Zhao H, et al. PET imaging of neovascularization with (68)Ga-3PRGD2 for assessing tumor early response to Endostar antiangiogenic therapy. *Mol Pharm.* 2014;11:3915–22.
  19. Bao X, Wang MW, Luo JM, Wang SY, Zhang YP, Zhang YJ. Optimization of early response monitoring and prediction of cancer antiangiogenesis therapy via noninvasive PET molecular imaging strategies of multifactorial bioparameters. *Theranostics.* 2016;6:2084–98.
  20. Yang G, Nie P, Kong Y, Sun H, Hou G, Han J. MicroPET imaging of tumor angiogenesis and monitoring on antiangiogenic therapy with an (18)F labeled RGD-based probe in SKOV-3 xenograft-bearing mice. *Tumour Biol.* 2015;36:3285–91.
  21. Yang M, Gao H, Yan Y, Sun X, Chen K, Quan Q, et al. PET imaging of early response to the tyrosine kinase inhibitor ZD4190. *Eur J Nucl Med Mol Imaging.* 2011;38:1237–47.
  22. Ji S, Zheng Y, Shao G, Zhou Y, Liu S. Integrin alpha(v)beta(3)-targeted radiotracer (99m)Tc-3P-RGD(2) useful for noninvasive monitoring of breast tumor response to antiangiogenic linifanib therapy but not anti-integrin alpha(v)beta(3) RGD(2) therapy. *Theranostics.* 2013;3:816–30.
  23. Minamimoto R, Karam A, Jamali M, Barkhodari A, Gambhir SS, Dorigo O, et al. Pilot prospective evaluation of (18)F-FPPRGD2 PET/CT in patients with cervical and ovarian cancer. *Eur J Nucl Med Mol Imaging.* 2016;43:1047–55.
  24. Strieth S, Eichhorn ME, Sutter A, Jonczyk A, Berghaus A, Dellian M. Antiangiogenic combination tumor therapy blocking alpha(v)-integrins and VEGF-receptor-2 increases therapeutic effects in vivo. *Int J Cancer.* 2006;119:423–31.
  25. Brooks PC, Montgomery AM, Rosenfeld M, Reisfeld RA, Hu T, Klier G, et al. Integrin alpha v beta 3 antagonists promote tumor regression by inducing apoptosis of angiogenic blood vessels. *Cell.* 1994;79:1157–64.
  26. Brooks PC, Clark RA, Chersesh DA. Requirement of vascular integrin alpha v beta 3 for angiogenesis. *Science.* 1994;264:569–71.
  27. Kumar CC. Integrin alpha v beta 3 as a therapeutic target for blocking tumor-induced angiogenesis. *Curr Drug Targets.* 2003;4:123–31.
  28. Stupack DG, Puente XS, Boutsaboualoy S, Storgard CM, Chersesh DA. Apoptosis of adherent cells by recruitment of caspase-8 to unligated integrins. *J Cell Biol.* 2001;155:459–70.
  29. Zhang H, Liu N, Gao S, Hu X, Zhao W, Tao R, et al. Can an (1)(8)F-ALF-NOTA-PRGD2 PET/CT scan predict treatment sensitivity to concurrent chemoradiotherapy in patients with newly diagnosed glioblastoma? *J Nucl Med.* 2016;57:524–9.
  30. Niu G, Chen X. RGD PET: from lesion detection to therapy response monitoring. *J Nucl Med.* 2016;57:501–2.